Supramolecular recognition of phosphodiester-based donor and acceptor oligomers forming gels in water

Kévan Pérez de Carvasal, Gérard Vergoten, Jean-Jacques Vasseur, Michael Smietana, François Morvan

▶ **To cite this version:**

Kévan Pérez de Carvasal, Gérard Vergoten, Jean-Jacques Vasseur, Michael Smietana, François Morvan. Supramolecular recognition of phosphodiester-based donor and acceptor oligomers forming gels in water. Biomacromolecules, 2023, 24 (2), pp.756-765. 10.1021/acs.biomac.2c01203 . hal-04120160

HAL Id: hal-04120160
https://hal.science/hal-04120160

Submitted on 7 Jun 2023

HAL is a multi-disciplinary open access archive for the deposit and dissemination of scientific research documents, whether they are published or not. The documents may come from teaching and research institutions in France or abroad, or from public or private research centers.

L'archive ouverte pluridisciplinaire **HAL**, est destinée au dépôt et à la diffusion de documents scientifiques de niveau recherche, publiés ou non, émanant des établissements d'enseignement et de recherche français ou étrangers, des laboratoires publics ou privés.

Supramolecular recognition of phosphodiester-based donor and acceptor oligomers forming gels in water

Kévan Pérez de Carvasal,† Gérard Vergoten,‡ Jean-Jacques Vasseur,† Michael Smietana,,† and François Morvan*,†*

†Université de Montpellier, CNRS, ENSCM, Institut des Biomolécules Max Mousseron, Montpellier, France.

‡Université de Lille, Inserm, INFINITE - U1286, Institut de Chimie Pharmaceutique Albert Lespagnol (ICPAL), Faculté de Pharmacie, 3 rue du Professeur Laguesse, 59006 Lille, France

ABSTRACT: Inspired by automated DNA synthesis, electron-rich dialkoxynaphthalene (DAN) donor and electron-deficient naphthalene-tetracarboxylic diimide (NDI) acceptor phosphodiester-linked homohexamers were synthesized by the phosphoramidite method. Two types of hexamers were prepared, one with only one phosphodiester between the aromatics (i.e. DAN or NDI) and a second with two phosphodiesters around a propanediol between the aromatics leading to the latter more flexible and more hydrophilic hexamers. The folding properties of these homohexamers alone or mixed together, in water only, were studied by UV-Visible absorption spectroscopy and

atomic force microscopy (AFM). AFM imaging revealed that 1:1 mixture of hexaDAN and hexaNDI formed fibers by charge transfer donor acceptor recognition leading to a hydrogel after drying. The organization of the resulting structures is strongly dependent on the nature of the complementary partner leading to the formation of mono- or multi-layers hydrogel networks with different compactness.

INTRODUCTION

The choice of a solvent in supramolecular assemblies[1] is a crucial parameter as it influences the recognition, folding and assembly capacity of the chosen units. The physical properties of water (polarity, solvation, hydrogen-bonding) lead to important modifications of the recognition phenomena governed by effects that are absent in other solvents. Consequently, supramolecular chemistry in water is singular and often challenging.[2] Supramolecular systems compatible with water[3, 4] have attracted a lot of interest,[5-7] and several studies increased the water solubility of large aromatic groups, with the introduction of charges[8-10] or hydrophilic functions.[11-14] Nevertheless most studies relied on organic solvents such as methanol, ethanol and DMSO to help solubilize and organize their systems and only few supramolecular assemblies were investigated in saline aqueous media or in water only.[15-21]

Among the interactions that guide supramolecular assemblies, charge transfer (CT) interaction implying aromatic electron donors and aromatic electron acceptors has been widely used[22] especially since it is generally intensified in water[23] and high polar protic solvents than in apolar solvents.[24-26]

Of the various supramolecular assemblies that can be generated from CT interactions, hydrogels[27] usually observed in AFM imaging as a xerogel after drying,[28-30] are particularly interesting for their applications,[31, 32] such as drug delivery systems,[33] antimicrobial agents for wounds[34] and matrix for bio-inspired artificial tissue engineering.[35] While there are many examples of hydrogen-bonded hydrogel networks,[36, 37] only a few studies described the production of hydrogels through charge transfer interactions in aqueous media.[38-43] CT interactions have many advantages providing not only self-assembly capacities but also recognition and selection properties.

We previously demonstrated that a negatively charged poly-phosphodiester heterohexamer, $P(DN)_3P$ composed of alternating aromatic dialkoxynaphthalene (DAN, D) donors and aromatic naphthalene diimide (NDI, N) acceptors and having propanediol ending arms (P) (Scheme 1), was able to fold into nanotubes in water with lengths of 400 nm to 1 µm depending on maturation times and concentration.[44] This heterohexamer was obtained by solid-supported DNA synthesis,[45, 46] from easily synthesized DAN and NDI phosphoramidite building blocks[44] (Fig.1A).

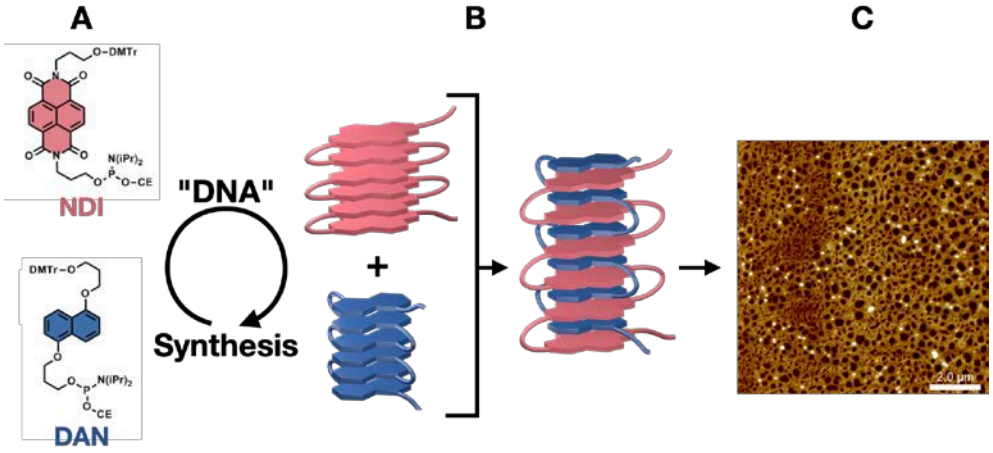

Figure 1. (A) Naphthalene diimide NDI and Dialkoxynaphthalene DAN phosphoramidite building blocks used for the synthesis of homohexamers with a DNA synthesizer, (B) Schematic representation of homohexamers assembly, (C) AFM imaging of the assembly depicted in (B) showing a network.

These results prompted us to investigate the duplex formation by CT interaction and the structuration of water-soluble homohexameric sequences composed of either DAN or NDI units linked by negatively charged phosphodiesters.[47] We demonstrate here that either alone or mixed together, these negatively charged short oligomers are able to form in water nanotubes or fibers leading to hydrogels after drying.

EXPERIMENTAL SECTION

Oligomers synthesis. The solid-supported synthesis of oligonucleotides was performed on a 394 ABI DNA synthesizer. All conventional CPG columns, reagents and solvents for DNA synthesis were purchased from Link© technologies, ChemGenes© Corporation and Biosolve© Chimie. The oligomers were elongated from the propanediol solid support, at 1 μmol scale, according to standard phosphoramidite chemistry protocols. The detritylation step was performed for 65 s using 3% TCA in CH_2Cl_2. For the coupling step, benzylmercaptotetrazole (0.3 M in anhydrous CH_3CN) was used as the activator with 1, 2 or 3 phosphoramidites (0.1 M in CH_3CN, 3 min coupling time). The capping step was performed with acetic anhydride using commercially available solutions (Cap A: acetic anhydride:pyridine:THF 10:10:80 v/v/v and Cap

B: 10% N-methylimidazole in THF) for 10 s. The oxidation step was performed with a standard, iodine solution (0.1 M I_2, THF:pyridine:water 90:5:5, v/v/v) for 15 s. Oligomers were deprotected and released from the CPG by treatment with a solution of 7 N NH_3/MeOH for 24 h with orbital agitation. WARNING: Treatment with concentrated aqueous ammonia leads to degradations due to the opening of the imides of NDI. The CPG beads were first washed with dry MeOH then with water. The two methanolic fractions were pooled and dried on a speed vacuum then the water fraction was added and dried too.

HPLC. Crude oligomers were purified by reversed-phase C_{18} HPLC (Macherey-Nagel, Nucleodur 250 x 10 mm, 5 µm) on a Thermo Fisher Ultimate 3000 system with a detector UV DAD 3000 at a flow rate of 4.5 mL/min. The conditions for the HPLC purification are reported in supplementary materials. The resulting oligomers with triethylammonium cations were exchanged on a DOWEX 50W X2 conditioned with Na^+ cation affording oligomers as sodium form which are more soluble in water. Reversed-phase C_{18} HPLC (Macherey-Nagel, Nucleodur 75x4,6 mm, 5 µm) analysis were performed on a Dionex Ultimate 3000 system with a detector UV DAD 3000 at a flow rate of 1 mL/min, with a gradient of 1% to 40% acetonitrile with 50 mM of TEAAc over 20 minutes.

Oligomers preparation and storage. The oligomers were stored dry at -20 °C to avoid structuration in water, then were dissolved at 0.1 mM in water to withdraw the needed number of nanomoles, this volume was then completed to 1 mL with water to obtain the needed concentration while the stock solution was reconditioned for storage. Then the solution was heated to 90 °C for 30 minutes, then cooled to 4 °C over 3 hours and kept at this temperature for 12 more hours.

Oligonucleotides characterization by MALDI-TOF. mass spectra were recorded on Axima© Assurance in negative mode, calibration was performed with a mixture of oligomers for reference, anthranilic acid was used as matrix. Oligomers (0.75 µL) were mixed with 1 µL of saturated solution of anthranilic acid in acetonitrile-water (1:1, v/v), this mixture was then deposed on a MALDI plate and dried.

UV-Visible study. UV-Vis spectra were recorded on a VARIAN© Cary 300 Bio UV-Vis spectrophotometer at 25 °C. All oligomers were dissolved at 15 µM in 1 mL of water for spectra analysis in an UV tank with 1 cm of path-length. Oligomers were heated to 90 °C for 30 minutes and slowly cooled to 25 °C to allow an optimized association before analysis.

AFM imaging study. Atomic force microscopy analyses were recorded using Nanoscope on three instruments: MultiMode 8 (Quantitative nanomecanics QNM) equipped with nanoscope V electronics in peak force mode. Bruker Dimension 3100 equipped with nanoscope IIIa quadrex electronics in tapping mode. Nanoman 5 equipped with nanoscope V electronics in tapping mode. We used 300-rtespa and Rfesp-75 probes from Bruker with a tip radius of 5 nm. The mica substrates of highest grade V1 mica discs 15 mm (Ted Pella, Inc., with a Rq equal to 0.09 nm) were attached to a steel baseplate with carbon tape. For each analysis 40 µL of the aqueous solution containing our oligomers were placed on a freshly cleaved mica surface and dried at room temperature for 30 minutes to 4 hours for the hydrogel structures in a laminar flow cabinet.

SEM imaging study. The study was performed on a FEI Quanta 200 FEG instrument from MEA platform, Université de Montpellier. The sample was deposited at 15 µM on a carbon ribbon and dried for 2h before analysis.

Supramolecular assembly dissociation. For total dissociation of supramolecular assembly, a treatment with 5 mg of SDS (sodium dodecylsulfate) in a 2 mL solution at 90 °C is performed for 30 minutes. After that 200 µL of a 2 M TEAAc buffer is added to the solution. The oligomer is then acquired using a C_{18} Sep-Pak system from Waters.

Molecular modelling. The structure of the arrangements has been optimized using a classical Monte Carlo conformational searching procedure as described in the BOSS software.[48] For that purpose, the Spectroscopic Empirical Potential Energy function SPASIBA and the corresponding parameters are used [49, 50] Molecular graphics and analysis were performed using the Discovery Studio 2020 Client software, Dassault Systemes Biovia Corp.

RESULTS AND DISCUSSION

Synthesis of monomers and hexamers of DAN and NDI. The homohexamers were synthesized at a classic DNA scale synthesis of 1 µmol using NDI (N), DAN (D) and propanediol (P) phosphoramidites starting from a propanediol solid support (Scheme 1, Fig. S1-4).[44] Three series of compounds were considered. The A series contains the monomers of DAN and NDI as PDP and PNP, and the alternated heterohexamer $P(DN)_3P$. They present at each end a propanediol phosphodiester moiety to increase their hydrosolubility. The B series concerns the homohexamers having six DAN as PD_6P or six NDI as PN_6P. In the C series, designed to probe the influences of flexibility, an additional propanediol negatively charged phosphodiester unit was placed after each DAN or NDI leading to homohexamers $P(DP)_6$ and $P(NP)_6$. Note that it also increased the number of negative charges and the global hydrophilicity of both hexamers.

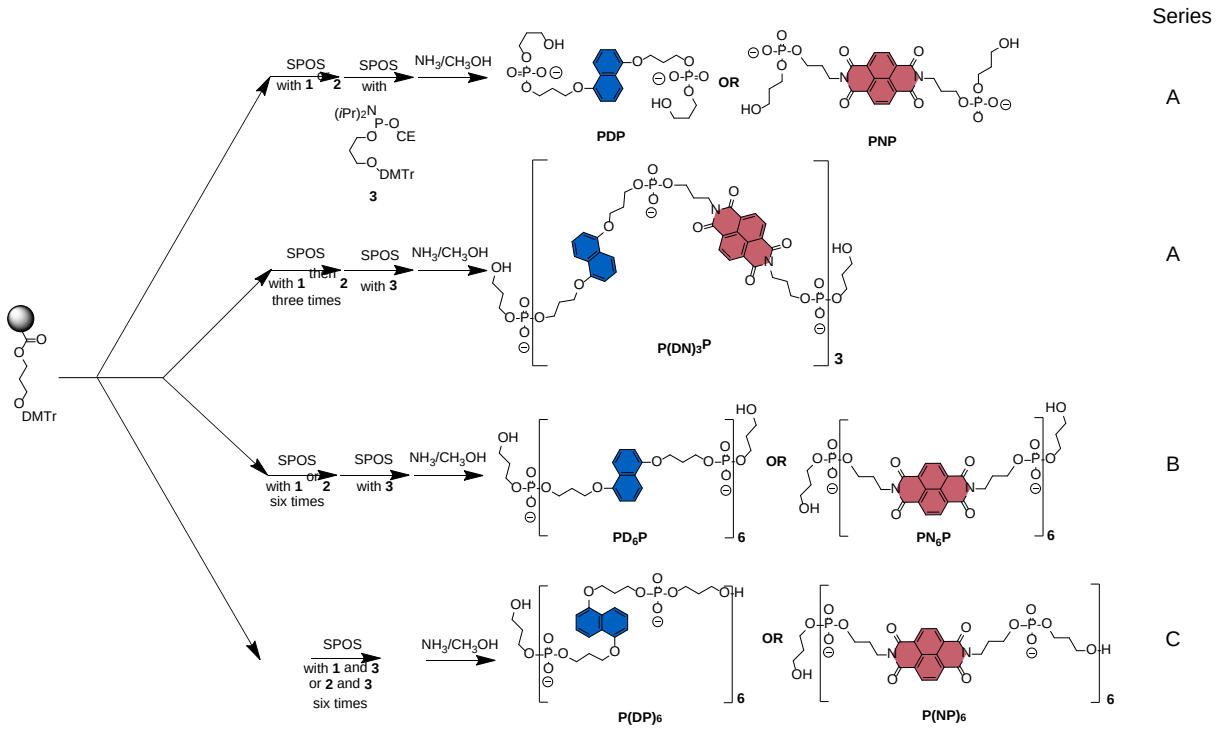

Scheme 1 Synthesis of monomers and hexamers of DAN and NDI.

UV-Visible study. All hexaDANs PD_6P and $P(DP)_6$, and the monomer PDP showed similar UV-Vis spectral properties. The characteristic bands of the dialkoxynaphtalene moiety at 284, 296, 311 and 324 nm present a good resolution and are well defined and separated (Fig. 2A). In contrast when DANs are involved in a CT interaction, i.e. $P(DN)_3P$, the bands are smoothed which gives a broadened band around 300 nm. Note that the molar concentration of monomers is equals to that of $P(DN)_3P$ but is twice lower than the hexamers. So, no significant hypochromicity was observed for the hexamers. The hexaNDIs PN_6P and $P(NP)_6$ presented identical spectra with two bands at 363 and 386 nm, the latter being of lower intensity, while the

opposite is observed with the monomer (Fig.2B).[8, 51-54] Finally, when NDIs are involved in a CT interaction (i.e. $P(DN)_3P$), a 37% hypochromicity was observed and both bands were broadened with a similar intensity, a slight red shift is also observable.[44] This variation of the NDIs bands intensities allowed to determine when NDI is monomeric, involved in a CT or in a stacked polyNDI interactions.[14, 55].

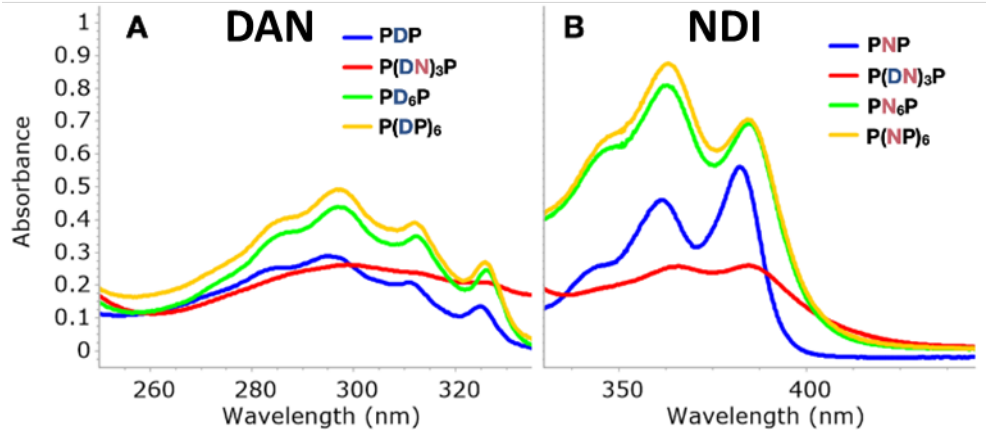

Figure 2. DAN (A) and NDI (B) based oligomers UV-Vis study in water, with PDP and PNP at 45 µM, and $P(DN)_3P$, PD_6P, PN_6P, $P(DP)_6$, $P(NP)_6$ at 15 µM.

We then studied the UV-Vis spectral properties of mixtures of homohexamers. The mixture of an equimolar quantity of a yellow solution of PN_6P with a colorless solution of PD_6P, instantly produced an intense pink solution visible to the naked-eye[52, 56-59] characteristic of the CT interaction and confirmed by the low intensity band centered around 540 nm. The UV-Vis spectrum showed for the NDI bands a broadening as well as a hypochromicity and a similar intensity (Fig. 3A). These data support the strong interaction between DAN and NDI aromatic units resulting from their intertwining recognition.[8, 53, 60]

In contrast, upon mixing an equimolar amount of $P(DP)_6$ and $P(NP)_6$, a weak-colored pink solution was observed as well as a faint CT band. In addition, NDI bands showed a stacked polyNDI pattern while DAN bands were unbroadened (Fig. 3B). These data suggest there was a weak or no intertwining between $P(DP)_6$ and $P(NP)_6$.

Both B and C series are composed of 6 aromatic units, but they differ by their number of negative charges (7 and 12, respectively). In addition, the higher hydrophilicity of the C series, demonstrated by the shorter retention time observed in RP HPLC analysis (Fig. S5), probably leads to a better solvation in water thus reducing the solvophobic effect. Consequently, the enhanced charge repulsion of the phosphodiester groups upon the mixing of C series hexamers, combined with a weak aromatic interaction and a higher entropic cost due to a higher flexibility, appears to have prevented strong intertwining of the aromatic units compared to the B series hexamers.

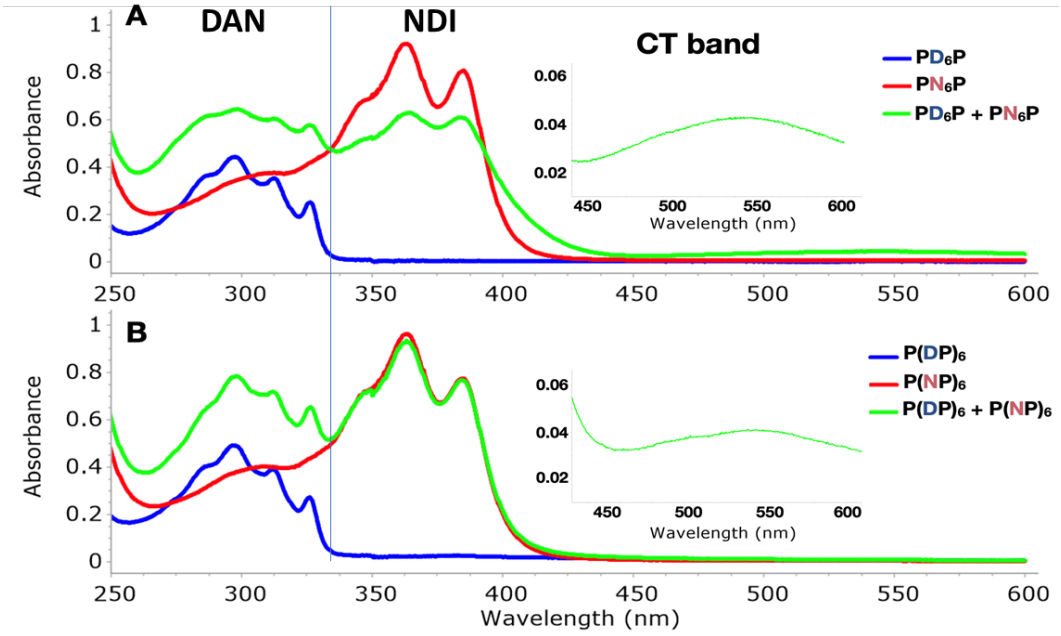

Figure 3. UV-Vis study at 15 µM in water of A) $P(D)_6P$, $P(N)_6P$, and their 1:1 mixture (inset zoom of CT band) and B) of $P(DP)_6$, $P(NP)_6$ and their 1:1 mixture (inset zoom of CT band at 30 µM.)

AFM study. Based on this observation, we hypothesized that supramolecular assemblies of a B-series mix would be denser than those of the C-series. To better understand these differences AFM imaging analyses were performed. TEM imaging cannot be performed because uranyl acetates induce a strong destabilization due to their high interaction with phosphodiesters.[61] Homohexamers were studied alone in water at 15 µM after a heat-cooling gradient and 12-hour of maturation allowing a better organization than in our previous study. PD_6P presented only few and small linear fibers of 1 nm height and tens to hundreds nm long with a wideness of 40 to 100 nm, thus suggesting a connection of multiple fibers next to each other (Fig. 4A). Häner observed a similar fiber formation with phosphodiester heptapyrenes.[62] By contrasts, PN_6P, due to strong NDI interactions in water,[24] led to a large porous network of different heights ranging from 1 to 6 nm, suggesting up to six layers of 1 nm with hole disparity ranging from 20 to 280 nm in diameter (Fig. 4C). $P(DP)_6$ also showed few fibers similar to the one observed with PD_6P with a height of 1.5 nm (Fig.4B), while $P(NP)_6$ showed, after drying, a monolayer xerogel honeycomb network with holes ranging from 30 to 240 nm in diameter with a height of 1.5 nm (Fig.4D). Compared to PN_6P, the observed difference of structure can be explained by a better solvation of $P(NP)_6$ in water leading to a lower solvophobic effect.[1] The denser structuration observed with homoNDI hexamers in comparison with $homoDAN_6$ is a consequence of lower electronic repulsion and thus an enhanced interaction in water between acceptors units.[1]

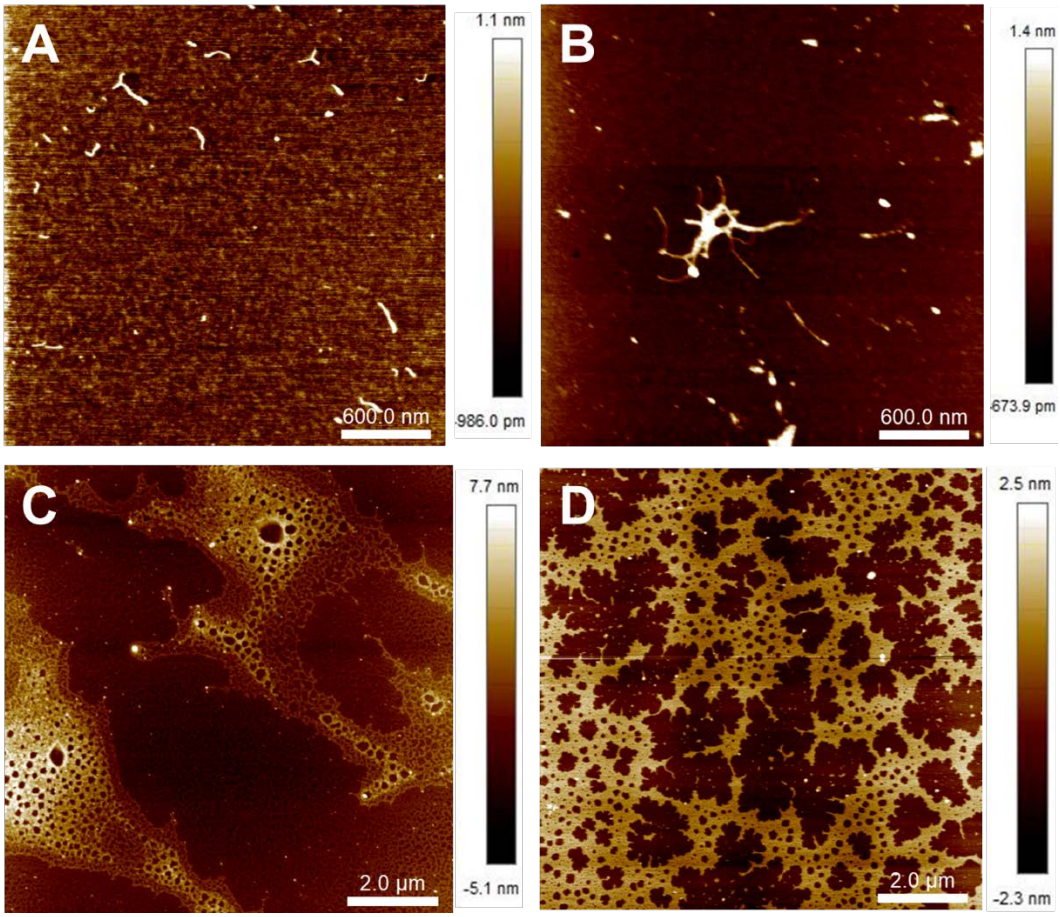

Figure 4. AFM images (height) at 15 µM in water of A) PD_6P, B) $P(DP)_6$, C) PN_6P and D) $P(NP)_6$.

We further investigated their structuring depending on the nature of a complementary partner, i.e. monomers or hexamers. First, each hexamer was mixed with its complementary monomer. Interestingly, a 1:6 mixture of PD_6P:PNP led to fibers of 400 to 900 nm in length, 22 nm wide and 1.2 nm in height (Fig. S6) and thus much longer than those observed with the hexamer alone. In contrast, a 1:6 mixture of $P(DP)_6$:PNP showed an irregular sheet of 1 or 2 nm in height (Fig. S7). The addition of 6 equivalents of PDP to PN_6P or $P(NP)_6$ gave for the former a dense and regular sheet 2 nm high (Fig. S8) and for the latter a more dispersed and irregular 3 nm high

sheet (Fig. S9). Thus, hydrophobic PD_6P and PN_6P hexamers formed structured nanotubes or a regular sheet assembly with their complementary monomers while the hydrophilic $P(DP)_6$ and $P(NP)_6$ hexamers led to more dispersed assemblies, probably due to a higher solvation in water leading to lower interactions.

Finally, all complementary hexamers were successively mixed together. The 1:1 mixture of the B and C series i.e. PD_6P:$P(NP)_6$ and PN_6P:$P(DP)_6$ led for the former to a dispersed and monolayered network averaging 1.6 nm high (Fig. 5A, S10) and for the latter a dense and monolayered network 2 nm high with hole disparity in the sheet ranging from 20 to 80 nm in diameter (Fig. 5B, S11).

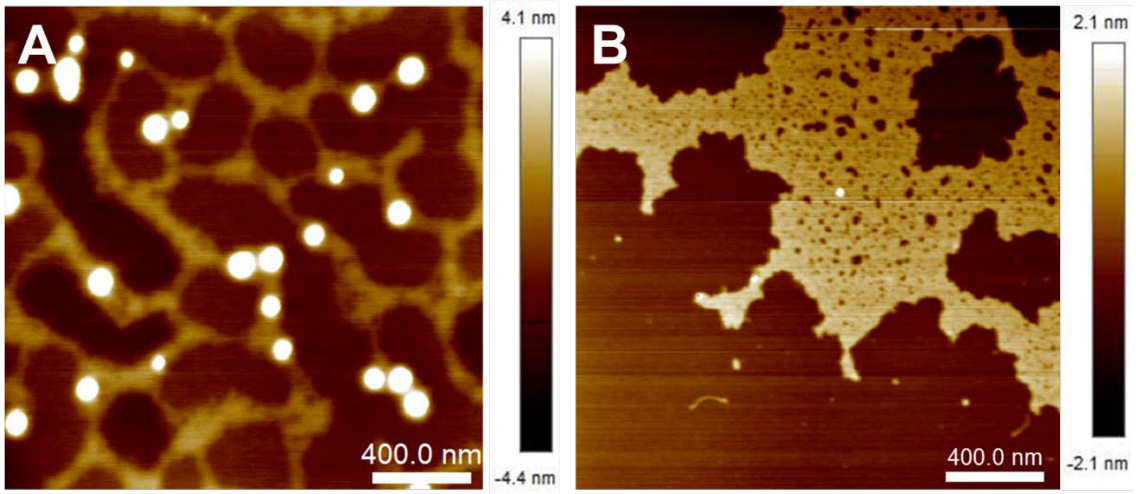

Figure 5. AFM images (height) in water of a 1:1 mixture at 15 µM for each hexamers A) PD_6P:$P(NP)_6$ and B) PN_6P:$P(DP)_6$.

Mixing an equimolar amount of PD_6P with PN_6P (Fig. 6A) revealed a dense and large porous honeycomb network 20 nm high, with holes ranging from 30 nm to 450 nm in diameter. The recognition between DAN and NDI motifs of these more hydrophobic hexamers allowed a homogenous structure resulting from the aggregation of the fibers (Fig. S13). It should also be noted that while the drying usually takes place within minutes, this sample required hours (Table S1), thus indicating a better retention of water in the holes of the network.

Then, mixing an equimolar amount of $P(DP)_6$ and $P(NP)_6$ led to a monolayer dendrimer network 2 nm high (Fig. 6B). This structure is characterized by a wideness ranging from 150 to 300 nm and is narrower than that the one obtained with $P(NP)_6$ alone thus confirming the recognition of both complementary hexamers.

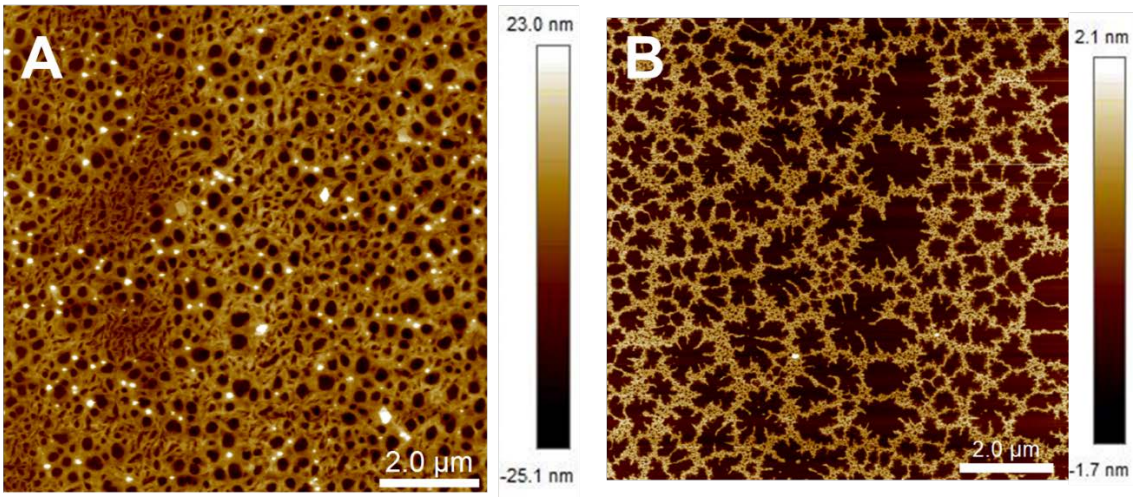

Figure 6. AFM images (height) in water of a 1:1 mixture at 15 µM for each hexamer of A) PD_6P:PN_6P and B) $P(DP)_6$:$P(NP)_6$.

As expected, the difference in the number of charges of the four mixtures led to four different systems. Indeed, the system with the most negative charge $P(DP)_6$:$P(NP)_6$ was also the most spread out because of the greater repulsion between the primary fibers, while the one with the least negative charges PN_6P and PD_6P showed the densest network. Another possibility to explain the lower efficiency of $P(NP)_6$ to recognize it complementary hexaDAN could be the formation of an anion-π pair between the NDI and the phosphodiester anion leading to a lower interaction with DAN moieties. Indeed, Matile reported the formation of anion-π between NDI and enolate or nitrolate.[63-68] Such anion-π interaction induced the formation of a CT band at 500 nm.[69] So, each hexaNDI was carefully studied by UV-visible spectroscopy at 15 µM at 4 and 80 °C. For each, the band at 363 nm was higher than that at 386 nm in agreement with the π–π stacking of NDIs and no CT band was visible around 500 nm that allowed us to exclude the formation of an anion-π interaction between NDI and phosphodiesters (Fig. S12).

Compared to the nanotubes formed with alternating DAN and NDI units such as $P(DN)_3P$[44] the mixture of homohexamers led to the formation of hydrogels from longer fibers interacting with each other (Fig. S13), and trapping water at the same time.[70]

The weak structural differences between $P(DN)_3P$ and PN_6P/PD_6P duplexes puzzled us as we anticipated that they would organize similarly. In fact, the conditions of the formation of the current structures in comparison with previously reported $P(DN)_3P$ were different. Indeed, in our first study the foldamer was dissolved in water at 25°C and then kept overnight at 4°C. In the current study the samples were dissolved in water, heated at 90 °C for 30 minutes, cooled to 4 °C over 3 hours (0.5°C/min) and then kept at 4°C overnight. So as a control $P(DN)_3P$ was treated as

the same way and AFM images showed the formation of a monolayer hydrogel 2 nm high with a high density (Fig. 7).

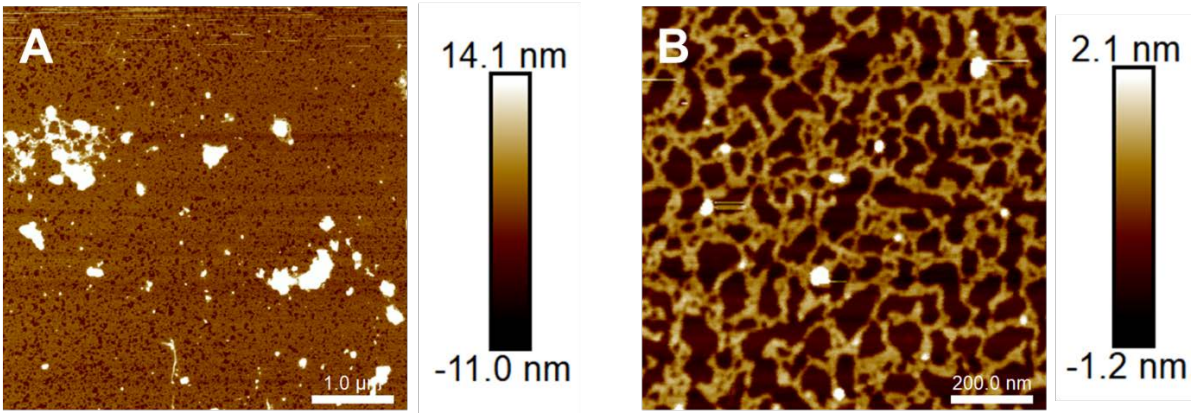

Figure 7. AFM images (height) in water of $P(DN)_3P$ at 15 µM prepared with a gradient of temperature (90°C to 4°C over 3h) and kept at 4°C overnight A) 5 µm wide image, B) 2 µm wide image.

As a further control, both PN_6P and PD_6P hexamers were just dissolved in water together at 25°C and cooled at 4°C and kept overnight at this temperature. In this case, AFM images showed the formation of a hydrogel with partially few layers with a higher density than that of $P(DN)_3P$ (Fig. 8). The difference of supramolecular arrangements according to the sample preparation has been previously reported by Häner.[71]

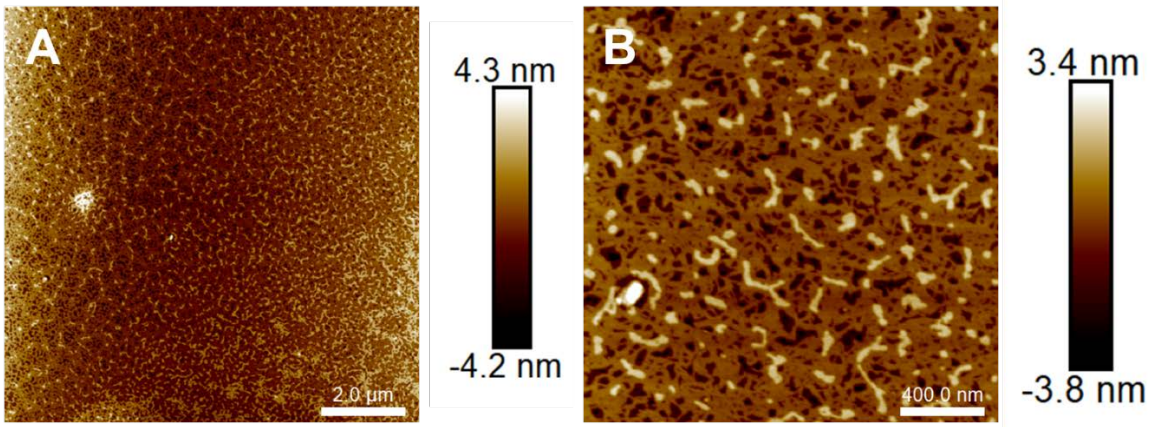

Figure 8. AFM images (height) in water of a 1:1 mixture at 15 µM of PD_6P:PN_6P prepared at 25°C and then 4°C overnight.

So, we can assume that the alternated foldamer $P(DN)_3P$ and the PN_6P:PD_6P duplex are both able to form a hydrogel depending on the preparation of the samples. However, the formation of fibers or nanotubes leading to the hydrogel, after drying, might follow different ways (Fig. 9). For the alternated foldamer, the supramolecular arrangement may be weaker since the assembly of terminal DAN and NDI could be reversed by heating as we previously demonstrated.[44] In the case of the PN_6P:PD_6P duplex, two types of arrangement can be foreseen. The first involves the formation of a blunt-ended duplex and a supramolecular arrangement driven by the assembly of terminal DAN and NDI units. The second implies the formation of long duplexes by concatenation of the hexamers. In the latter case the stability of the structure would be more stable. This difference of behavior may explain the differences of supramolecular arrangements observed with the formation of a hydrogel for the PN_6P:PD_6P duplex independent of the conditions of preparation of the sample.

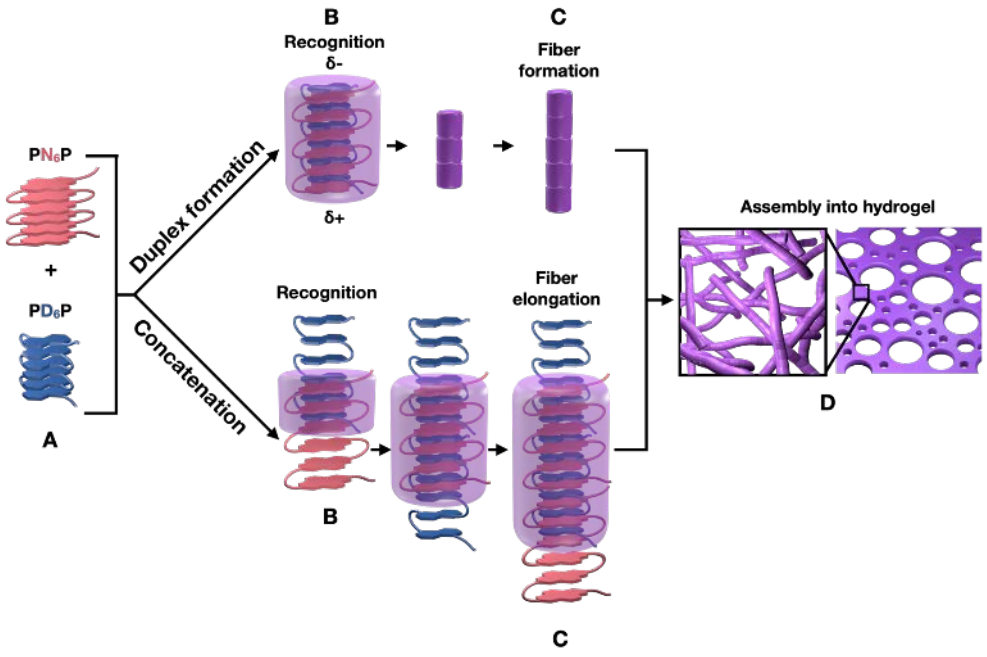

Figure 9. Illustration of the two ways the hexamers mixture is able to form a hydrogel by DAN/NDI recognition. A) Homohexamers mixture B) Foldamer intertwining C) Fiber formation and D) Hydrogel assembly.

Molecular modelling study. A molecular modelling study was performed to envision the arrangement of the homohexamers alone or as a duplex (Fig.S20-S28). For each structure, we calculated the average value of the distance between two phosphorus atoms on either side of an aromatic ring (PP) or between two central methylenes of the propanol linkers (CC), the distance between two aromatic units and the length of each structure (Table 1). HexaDANs stacked by π–π interactions led to DAN motifs in line with the phosphodiesters on the sides. The distance between DANs is higher for $P(DP)_6$ (3.8 Å vs. 3.2 Å) probably due to its greater flexibility. While hexaNDIs also stacked by π–π interaction showed more regular structures with the same distance between NDIs (3.2 Å) probably due to the stronger NDI-NDI interaction. The molecular

modelling of duplexes showed DAN/NDI alternated structures similar to DNA duplexes with the aromatic motifs in the middle and the phosphodiesters on the sides, and a distance between DAN and NDI ranging from 3.4 to 3.8 Å. The PP and CC distances of duplex are slightly lower than for the hexamers alone due to the stretching by the insertion of the DAN and NDI motifs to form alternated structures. The structure of the duplexes formed by recognition of complementary DAN and NDI is similar to that observed for the alternated foldamer $P(DN)_3P$ with similar PP distances but the duplexes show less compact structures with a higher distance between DAN and NDI.

Table 1 Average distances between phosphorous atoms (PP), central methylenes (CC) and DAN or NDI aromatic motifs (arom/arom) and length of the different hexamers alone or in duplex.

Structures	Distance in Å					
	PP_{DAN}	CC_{DAN}	PP_{NDI}	CC_{NDI}	arom/arom	Length
PD_6P	15.0				3.2	19.0
$P(DP)_6$		20.1			3.8	19.9
PN_6P			16.3		3.2	17.8
$P(NP)_6$				21.4	3.2	17.8
$P(DP)_6/PN_6P$		15.1	15.7		3.7	38.7
$PD_6P/P(NP)_6$	14.5			17.8	3.4	36.4
PD_6P/PN_6P	14.6		15.8		3.8	38.7
$P(DP)_6/P(NP)_6$		16.4		20.4	3.6	39.3
$P(DN)_3P$	14.4		15.8		3.2	16.1

In figure 10, for the PN_6P/PD_6P duplex, only three NDI and DAN motifs are shown for ease of comparison (Fig. S25). The duplex shows a very similar arrangement compared to the hetero foldamer with a distance between two aromatics of about 3.5 Å and a width of about 1.6 nm wide.

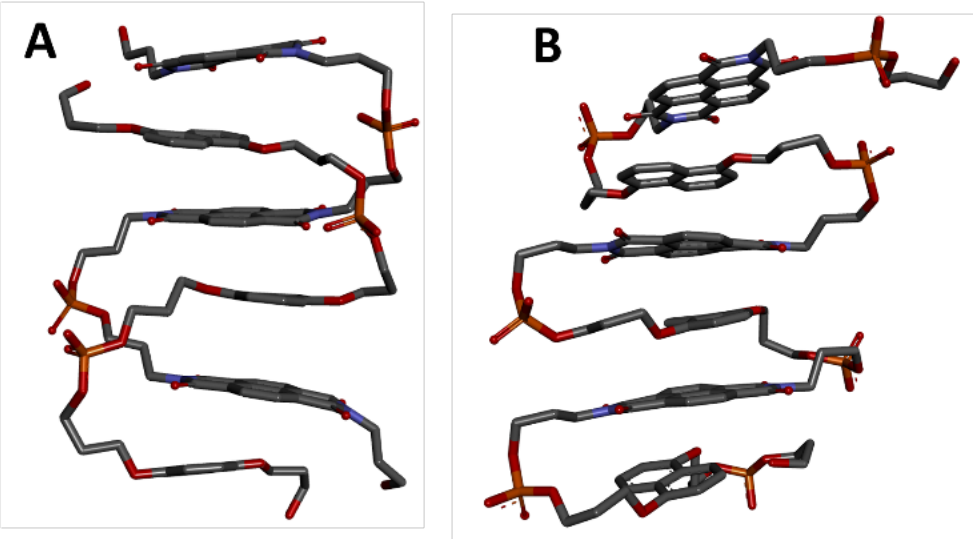

Figure 10 Modelling of the assembly of A) PD_6P/PN_6P, only three NDI and DAN motifs are shown for ease of comparison with B) $P(DN)_3P$.

CONCLUSIONS

In summary, phosphodiester-based homohexamers of DAN and NDI were easily synthesized by solid-supported DNA synthesis. By recognition of DAN and NDI motifs, the homohexamers were able to bind in water by charge transfer interaction exhibiting a CT band at 540 nm of low

intensity. In addition, we showed that the behavior of the two NDI motif bands at 363 and 386 nm is also a signature of the recognition with the DAN motif. A large variety of structures could be obtained from these hexamers from the formation of nanotubes to various types of hydrogel networks after drying. While additional negative charges in the hexamers increase their water solubility, they also influence their structuring in a detrimental way. From a simplistic point of view, the lowest association strength was observed for the hexamers that exhibited the best solvation in water due to excess of charge repulsion and a lower solvophobic effect. In addition, the introduction of additional charge is associated with a higher flexibility inducing a higher entropic cost. The less hydrophilic PD_6P:PN_6P mixture formed a dense and thick honeycomb hydrogel of 20 nm in height while the more hydrophilic mixes of hexamers formed irregular monolayer networks 2-3 nm in height. A SEM study of 1 :1 mixture of PN_6P:PD_6P showed the formation of supramolecular fibrillar polymers in agreement with the formation of gels (Fig S29). These results demonstrate the delicate balance between water solubility, flexibility and lipophilicity for the assembly by recognition of supramolecular structures such as nanotubes and hydrogels. Hydrogels and water-soluble gel networks are currently being extensively studied for their use as biocompatible materials. Hydrogels formed with DNA are largely reported in the literature.[72, 73]. Usually, these hydrogels are formed by hybridization of DNA Y-shaped structures or DNA-grafted polymers with a complementary DNA sequence leading to a network. In the current hydrogels, we showed that short sequences with only six units are able to form hydrogels by supramolecular arrangement strongly stabilized by CT of the DAN and NDI pairs. Since these are the first charge transfer stabilized oligomers to yield a hydrogel in water, these new data shed new light in this area, further expanding the field of hydrogels formed by CT

recognition in water. However, additional studies will be carried out to better understand the behavior of this new supramolecular arrangements in water.

ASSOCIATED CONTENT

Supporting Information.

The following files are available free of charge.

HPLC profiles and MALDI-TOF spectra of hexamers. AFM images and molecular modeling of duplexes.

AUTHOR INFORMATION

Corresponding Authors

E-mail: François Morvan (francois.morvan@umontpellier.fr) and Michael Smietana (michael.smietana@umontpellier.fr).

ORCID

Kévan Pérez de Carvasal: 0000-0002-9271-4865

Gérard Vergoten: 0000-0001-6336-3923

Jean-Jacques Vasseur: 0000-0002-4379-6139

Michael Smietana: 0000-0001-8132-7221

François Morvan: 0000-0001-5077-0028

Author Contributions

The manuscript was written through contributions of all authors. All authors have given approval to the final version of the manuscript.

Notes

The authors declare no competing financial interest.

ACKNOWLEDGMENT

K. Pérez de Carvasal thanks the University of Montpellier (UM) for the award of a research studentship. F. Morvan is a member of Inserm. We thank Dr David Canevet (University of Angers) for critical discussion. We thank Dr. F. Menges (University of Konstanz) for the use of Spectragryph software. We thank the Centrale de Technologie en Micro et nanoélectronique of UM for AFM analyses and F. Fernandez from the MEA platform, Université de Montpellier, for the SEM experiments.

REFERENCES

(1) Wurthner, F. Solvent Effects in Supramolecular Chemistry: Linear Free Energy Relationships for Common Intermolecular Interactions. *J. Org. Chem.* **2022**, *87*, 1602-1615.
(2) Spitzer, D.; Besenius, P. Aqueous Supramolecular Polymers and Hydrogels. In *Supramolecular Chemistry in Water*, Wiley, 2019; pp 285-336.
(3) Oshovsky, G. V.; Reinhoudt, D. N.; Verboom, W. Supramolecular chemistry in water. *Angew Chem Int Ed Engl* **2007**, *46*, 2366-2393.
(4) Krieg, E.; Bastings, M. M. C.; Besenius, P.; Rybtchinski, B. Supramolecular Polymers in Aqueous Media. *Chem. Rev.* **2016**, *116*, 2414-2477.
(5) Iwaura, R.; Yoshida, K.; Masuda, M.; Ohnishi-Kameyama, M.; Yoshida, M.; Shimizu, T. Oligonucleotide-templated self-assembly of nucleotide bolaamphiphiles: DNA-like nanofibers edged by a double-helical arrangement of A-T base pairs. *Angew Chem Int Ed Engl* **2003**, *42*, 1009-1012.
(6) Tomasulo, M.; Naistat, D. M.; White, A. J. P.; Williams, D. J.; Raymo, F. M. Self-assembly of naphthalene diimides into cylindrical microstructures. *Tetrahedron Lett.* **2005**, *46*, 5695-5698.
(7) Iwaura, R.; Shimizu, T. Reversible photochemical conversion of helicity in self-assembled nanofibers from a 1,omega-thymidylic acid appended bolaamphiphile. *Angew Chem Int Ed Engl* **2006**, *45*, 4601-4604.

(8) Lokey, R. S.; Iverson, B. L. Synthetic molecules that fold into a pleated secondary structure in solution. *Nature* **1995**, *375*, 303-305.
(9) Bosch, C. D.; Jevric, J.; Burki, N.; Probst, M.; Langenegger, S. M.; Haner, R. Supramolecular Assembly of DNA-Phenanthrene Conjugates into Vesicles with Light-Harvesting Properties. *Bioconjugate Chem.* **2018**, *29*, 1505-1509.
(10) Rothenbuhler, S.; Bosch, C. D.; Langenegger, S. M.; Liu, S. X.; Haner, R. Self-assembly of a redox-active bolaamphiphile into supramolecular vesicles. *Org. Biomol. Chem.* **2018**, *16*, 6886-6889.
(11) Bigot, J.; Charleux, B.; Cooke, G.; Delattre, F.; Fournier, D.; Lyskawa, J.; Sambe, L.; Stoffelbach, F.; Woisel, P. Tetrathiafulvalene End-Functionalized Poly(N-isopropylacrylamide): A New Class of Amphiphilic Polymer for the Creation of ultistimuli Responsive Micelles. *J. Am. Chem. Soc.* **2010**, *132*, 10796-10801.
(12) Jouault, N.; Xiang, Y.; Moulin, E.; Fuks, G.; Giuseppone, N.; Buhler, E. Hierarchical supramolecular structuring and dynamical properties of water soluble polyethylene glycol-perylene self-assemblies. *Phys. Chem. Chem. Phys.* **2012**, *14*, 5718-5728.
(13) Appukutti, N.; Serpell, C. J. High definition polyphosphoesters: between nucleic acids and plastics. *Polym. Chem.* **2018**, *9*, 2210-2226.
(14) Choisnet, T.; Canevet, D.; Salle, M.; Nicol, E.; Niepceron, F.; Jestin, J.; Colombani, O. Robust supramolecular nanocylinders of naphthalene diimide in water. *Chem. Commun.* **2019**, *55*, 9519-9522.
(15) Abe, H.; Mawatari, Y.; Teraoka, H.; Fujimoto, K.; Inouye, M. Synthesis and Molecular Recognition of Pyrenophanes with Polycationic or Amphiphilic Functionalities: Artificial Plate-Shaped Cavitant Incorporating Arenes and Nucleotides in Water. *J. Org. Chem.* **2004**, *69*, 495-504.
(16) Lagona, J.; Wagner, B. D.; Isaacs, L. Molecular-Recognition Properties of a Water-Soluble Cucurbit[6]uril Analogue. *J. Org. Chem.* **2006**, *71*, 1181-1190.
(17) Fang, L.; Basu, S.; Sue, C.-H.; Fahrenbach, A. C.; Stoddart, J. F. Syntheses and Dynamics of Donor−Acceptor [2]Catenanes in Water. *J. Am. Chem. Soc.* **2011**, *133*, 396-399.
(18) Draper, E. R.; Eden, E. G.; McDonald, T. O.; Adams, D. J. Spatially resolved multicomponent gels. *Nat. Chem.* **2015**, *7*, 848-852.
(19) Cougnon, F. B. L.; Ponnuswamy, N.; Pantoş, G. D.; Sanders, J. K. M. Molecular motion of donor–acceptor catenanes in water. *Org. Biomol. Chem.* **2015**, *13*, 2927-2930.
(20) Vybornyi, M.; Vyborna, Y.; Häner, R. DNA-inspired oligomers: from oligophosphates to functional materials. *Chem. Soc. Rev.* **2019**, *48*, 4347-4360.
(21) Asanuma, H.; Murayama, K.; Kamiya, Y.; Kashida, H. The DNA Duplex as an Aqueous One-Dimensional Soft Crystal Scaffold for Photochemistry. *Bull. Chem. Soc. Jpn.* **2018**, *91*, 1739-1748.
(22) Das, A.; Ghosh, S. Supramolecular assemblies by charge-transfer interactions between donor and acceptor chromophores. *Angew. Chem. Int. Ed.* **2014**, *53*, 2038-2054.
(23) Gabriel, G. J.; Iverson, B. L. Aromatic oligomers that form hetero duplexes in aqueous solution. *J. Am. Chem. Soc.* **2002**, *124*, 15174-15175.
(24) Cubberley, M. S.; Iverson, B. L. 1H NMR Investigation of Solvent Effects in Aromatic Stacking Interactions. *J. Am. Chem. Soc.* **2001**, *123*, 7560-7563.
(25) Winiger, C. B.; Langenegger, S. M.; Khorev, O.; Haner, R. Influence of perylenediimide-pyrene supramolecular interactions on the stability of DNA-based hybrids: Importance of electrostatic complementarity. *Beilstein J. Org. Chem.* **2014**, *10*, 1589-1595.

(26) Perez de Carvasal, K.; Riccardi, C.; Russo Krauss, I.; Cavasso, D.; Vasseur, J. J.; Smietana, M.; Morvan, F.; Montesarchio, D. Charge-Transfer Interactions Stabilize G-Quadruplex-Forming Thrombin Binding Aptamers and Can Improve Their Anticoagulant Activity. *Int. J. Mol. Sci.* **2021**, *22*, 9510-9533.
(27) Peak, C. W.; Wilker, J. J.; Schmidt, G. A review on tough and sticky hydrogels. *Colloid. Polym. Sci.* **2013**, *291*, 2031-2047.
(28) Yu, X.; Xie, D.; Lan, H.; Li, Y.; Zhen, X.; Ren, J.; Yi, T. Effect of water on the supramolecular assembly and functionality of a naphthalimide derivative: tunable honeycomb structure with mechanochromic properties. *J. Mater. Chem. C* **2017**, *5*, 5910-5916.
(29) Bieser, A. M.; Tiller, J. C. Surface-induced hydrogelation. *Chem. Commun.* **2005**, 3942-3944.
(30) Bieser, A. M.; Tiller, J. C. Structure and properties of an exceptional low molecular weight hydrogelator. *J Phys Chem B* **2007**, *111*, 13180-13187.
(31) Du, X.; Zhou, J.; Shi, J.; Xu, B. Supramolecular Hydrogelators and Hydrogels: From Soft Matter to Molecular Biomaterials. *Chem. Rev.* **2015**, *115*, 13165-13307.
(32) Fu, J.; In Het Panhuis, M. Hydrogel properties and applications. *J. Mater. Chem. B* **2019**, *7*, 1523-1525.
(33) Fu, L. H.; Qi, C.; Ma, M. G.; Wan, P. Multifunctional cellulose-based hydrogels for biomedical applications. *J. Mater. Chem. B* **2019**, *7*, 1541-1562.
(34) Yang, K.; Han, Q.; Chen, B.; Zheng, Y.; Zhang, K.; Li, Q.; Wang, J. Antimicrobial hydrogels: promising materials for medical application. *Int J Nanomedicine* **2018**, *13*, 2217-2263.
(35) Kim, J.; Shim, I. K.; Hwang, D. G.; Lee, Y. N.; Kim, M.; Kim, H.; Kim, S. W.; Lee, S.; Kim, S. C.; Cho, D. W.; et al. 3D cell printing of islet-laden pancreatic tissue-derived extracellular matrix bioink constructs for enhancing pancreatic functions. *J. Mater. Chem. B* **2019**, *7*, 1773-1781.
(36) Kameta, N.; Yoshida, K.; Masuda, M.; Shimizu, T. Supramolecular Nanotube Hydrogels: Remarkable Resistance Effect of Confined Proteins to Denaturants. *Chem. Mater.* **2009**, *21*, 5892-5898.
(37) Du, X.; Zhou, J.; Xu, B. Supramolecular hydrogels made of basic biological building blocks. *Chem. Asian. J.* **2014**, *9*, 1446-1472.
(38) Rao, K. V.; George, S. J. Supramolecular Alternate Co-Assembly through a Non-Covalent Amphiphilic Design: Conducting Nanotubes with a Mixed D–A Structure. *Chem. Eur. J.* **2012**, *18*, 14286-14291.
(39) Bhattacharjee, S.; Bhattacharya, S. Charge transfer induces formation of stimuli-responsive, chiral, cohesive vesicles-on-a-string that eventually turn into a hydrogel. *Chem. Asian. J.* **2015**, *10*, 572-580.
(40) Berdugo, C.; Nalluri, S. K.; Javid, N.; Escuder, B.; Miravet, J. F.; Ulijn, R. V. Dynamic Peptide Library for the Discovery of Charge Transfer Hydrogels. *ACS Appl Mater Interfaces* **2015**, *7*, 25946-25954.
(41) Bhattacharjee, S.; Maiti, B.; Bhattacharya, S. First report of charge-transfer induced heat-set hydrogel. Structural insights and remarkable properties. *Nanoscale* **2016**, *8*, 11224-11233.
(42) Gao, L.; Gao, Y.; Lin, Y.; Ju, Y.; Yang, S.; Hu, J. A Charge-Transfer-Induced Self-Healing Supramolecular Hydrogel. *Chem. Asian. J.* **2016**, *11*, 3430-3435.

(43) Biswakarma, D.; Dey, N.; Bhattacharya, S. A two-component charge transfer hydrogel with excellent sensitivity towards the microenvironment: a responsive platform for biogenic thiols. *Soft Matter* **2020**, *16*, 9882-9889.
(44) Perez de Carvasal, K.; Aissaoui, N.; Vergoten, G.; Bellot, G.; Vasseur, J. J.; Smietana, M.; Morvan, F. Folding of phosphodiester-linked donor-acceptor oligomers into supramolecular nanotubes in water. *Chem. Commun.* **2021**, *57*, 4130-4133.
(45) Beaucage, S. L.; Caruthers, M. H. Deoxynucleoside phosphoramidites—A new class of key intermediates for deoxypolynucleotide synthesis. *Tetrahedron Lett.* **1981**, *22*, 1859-1862.
(46) Roy, S.; Caruthers, M. Synthesis of DNA/RNA and their analogs via phosphoramidite and H-phosphonate chemistries. *Molecules* **2013**, *18*, 14268-14284.
(47) Appukutti, N.; de Vries, A. H.; Gudeangadi, P. G.; Claringbold, B. R.; Garrett, M. D.; Reithofer, M. R.; Serpell, C. J. Sequence-complementarity dependent co-assembly of phosphodiester-linked aromatic donor-acceptor trimers. *Chem. Commun.* **2022**, *58*, 12200-12203.
(48) Jorgensen, W. L.; Tirado-Rives, J. Molecular modeling of organic and biomolecular systems using BOSS and MCPRO. *J. Comput. Chem.* **2005**, *26*, 1689-1700.
(49) Lagant, P.; Nolde, D.; Stote, R.; Vergoten, G.; Karplus, M. Increasing normal modes analysis accuracy: The SPASIBA spectroscopic force field introduced into the CHARMM program. *J. Phys. Chem. A* **2004**, *108*, 4019-4029.
(50) Vergoten, G.; Mazur, I.; Lagant, P.; Michalski, J. C.; Zanetta, J. P. The SPASIBA force field as an essential tool for studying the structure and dynamics of saccharides. *Biochimie* **2003**, *85*, 65-73.
(51) Zych, A. J.; Iverson, B. L. Synthesis and Conformational Characterization of Tethered, Self-Complexing 1,5-Dialkoxynaphthalene/1,4,5,8-Naphthalenetetracarboxylic Diimide Systems. *J. Am. Chem. Soc.* **2000**, *122*, 8898-8909.
(52) Bradford, V. J.; Iverson, B. L. Amyloid-like Behavior in Abiotic, Amphiphilic Foldamers. *J. Am. Chem. Soc.* **2008**, *130*, 1517-1524.
(53) Molla, M. R.; Das, A.; Ghosh, S. Self-Sorted Assembly in a Mixture of Donor and Acceptor Chromophores. *Chem. Eur. J.* **2010**, *16*, 10084-10093.
(54) Das, A.; Ghosh, S. A generalized supramolecular strategy for self-sorted assembly between donor and acceptor gelators. *Chem. Commun.* **2011**, *47*, 8922-8924.
(55) Choudhury, P.; Das, K.; Das, P. K. l-Phenylalanine-Tethered, Naphthalene Diimide-Based, Aggregation-Induced, Green-Emitting Organic Nanoparticles. *Langmuir* **2017**, *33*, 4500-4510.
(56) Molla, M. R.; Das, A.; Ghosh, S. Chiral induction by helical neighbour: spectroscopic visualization of macroscopic-interaction among self-sorted donor and acceptor π-stacks. *Chem. Commun.* **2011**, *47*, 8934-8936.
(57) Singha, N.; Gupta, P.; Pramanik, B.; Ahmed, S.; Dasgupta, A.; Ukil, A.; Das, D. Hydrogelation of a Naphthalene Diimide Appended Peptide Amphiphile and Its Application in Cell Imaging and Intracellular pH Sensing. *Biomacromolecules* **2017**, *18*, 3630-3641.
(58) Dey, N. Naked-eye sensing of phytic acid at sub-nanomolar levels in 100% water medium by a charge transfer complex derived from off-the-shelf ingredients. *Analyst* **2020**, *145*, 4937-4941.
(59) Choisnet, T.; Canevet, D.; Salle, M.; Lorthioir, C.; Bouteiller, L.; Woisel, P.; Niepceron, F.; Nicol, E.; Colombani, O. Colored Janus Nanocylinders Driven by Supramolecular Coassembly of Donor and Acceptor Building Blocks. *ACS Nano* **2021**, *15*, 2569-2577.

(60) Peebles, C.; Piland, R.; Iverson, B. L. More than Meets the Eye: Conformational Switching of a Stacked Dialkoxynaphthalene–Naphthalenetetracarboxylic diimide (DAN–NDI) Foldamer to an NDI–NDI Fibril Aggregate. *Chem. Eur. J.* **2013**, *19*, 11598-11602.
(61) Watson , M. L. Staining of Tissue Sections for Electron Microscopy with Heavy Metals. *J. Biophys. Biochem. Cytol.* **1958**, *4*, 475-478.
(62) Vyborna, Y.; Altunbas, S.; Vybornyi, M.; Haner, R. Morphological diversity of supramolecular polymers of DNA-containing oligopyrenes-formation of chiroptically active nanosheets. *Chem. Commun.* **2017**, *53*, 12128-12131.
(63) Zhao, Y.; Cotelle, Y.; Avestro, A. J.; Sakai, N.; Matile, S. Asymmetric Anion-pi Catalysis: Enamine Addition to Nitroolefins on pi-Acidic Surfaces. *J. Am. Chem. Soc.* **2015**, *137*, 11582-11585.
(64) Cotelle, Y.; Benz, S.; Avestro, A. J.; Ward, T. R.; Sakai, N.; Matile, S. Anion-pi Catalysis of Enolate Chemistry: Rigidified Leonard Turns as a General Motif to Run Reactions on Aromatic Surfaces. *Angew Chem Int Ed Engl* **2016**, *55*, 4275-4279.
(65) Zhao, Y.; Cotelle, Y.; Sakai, N.; Matile, S. Unorthodox Interactions at Work. *J. Am. Chem. Soc.* **2016**, *138*, 4270-4277.
(66) Liu, L.; Cotelle, Y.; Avestro, A. J.; Sakai, N.; Matile, S. Asymmetric Anion-pi Catalysis of Iminium/Nitroaldol Cascades To Form Cyclohexane Rings with Five Stereogenic Centers Directly on pi-Acidic Surfaces. *J. Am. Chem. Soc.* **2016**, *138*, 7876-7879.
(67) Liu, L.; Cotelle, Y.; Bornhof, A. B.; Besnard, C.; Sakai, N.; Matile, S. Anion-pi Catalysis of Diels-Alder Reactions. *Angew Chem Int Ed Engl* **2017**, *56*, 13066-13069.
(68) Liu, L.; Cotelle, Y.; Klehr, J.; Sakai, N.; Ward, T. R.; Matile, S. Anion-pi catalysis: bicyclic products with four contiguous stereogenic centers from otherwise elusive diastereospecific domino reactions on pi-acidic surfaces. *Chem. Sci.* **2017**, *8*, 3770-3774.
(69) Dawson, R. E.; Hennig, A.; Weimann, D. P.; Emery, D.; Ravikumar, V.; Montenegro, J.; Takeuchi, T.; Gabutti, S.; Mayor, M.; Mareda, J.; et al. Experimental evidence for the functional relevance of anion–π interactions. *Nat. Chem.* **2010**, *2*, 533-538.
(70) Kleinsmann, A. J.; Nachtsheim, B. J. Phenylalanine-containing cyclic dipeptides – the lowest molecular weight hydrogelators based on unmodified proteinogenic amino acids. *Chem. Commun.* **2013**, *49*, 7818-7820.
(71) Vybornyi, M.; Rudnev, A.; Häner, R. Assembly of Extra-Large Nanosheets by Supramolecular Polymerization of Amphiphilic Pyrene Oligomers in Aqueous Solution. *Chem. Mater.* **2015**, *27*, 1426-1431.
(72) Li, F.; Tang, J.; Geng, J.; Luo, D.; Yang, D. Polymeric DNA hydrogel: Design, synthesis and applications. *Prog. Polym. Sci.* **2019**, *98*, 101163.
(73) Jian, X. T.; Feng, X. Y.; Luo, Y. N.; Li, F. J.; Tan, J. Y.; Yin, Y. L.; Liu, Y. Development, Preparation, and Biomedical Applications of DNA-Based Hydrogels. *Front. Bioeng. Biotechnol.* **2021**, *9*, 661409.

SYNOPSIS.

Supramolecular recognition of phosphodiester-based donor and acceptor oligomers forming gels in water

Kévan Pérez de Carvasal, Gérard Vergoten, Jean-Jacques Vasseur, Michael Smietana, and François Morvan

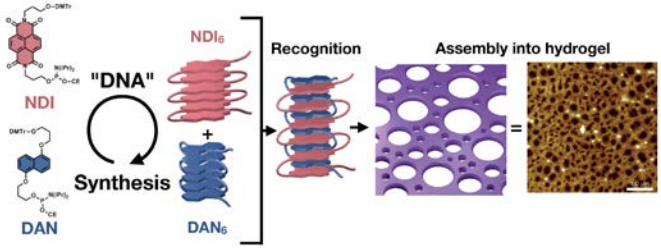

Duplexes of DNA-inspired homohexamers of the aromatic donor DAN and acceptor NDI form nanotubes or fibers by recognition and charge transfer interactions leading to a hydrogel after drying.